Fachtagung "Lasermethoden in der Strömungsmesstechnik"
6. – 8. September 2015, Cottbus

PIV-measurements on the momentum transfer in the forest edge region during extreme gusts

PIV-Messungen zum Impulstransfer in der Waldkantenregion während Extremböen

Christof Gromke*, Bodo Ruck
Laboratory of Building- and Environmental Aerodynamics, Institute for Hydromechanics, Karlsruhe Institute of Technology KIT, Karlsruhe, Germany
*gromke@kit.edu

Key words: vegetative canopy flow, forest edge, gust, storm stability, PIV
Schlagworte: Strömung in/um Vegetation, Waldkante, Böe, Sturmstabilität, PIV

Abstract

The flow phenomena above a forest and the associated downward momentum transport into the canopy were studied for an atmospheric boundary layer flow in combination with superimposed extreme gusts. Forest stands with two types of windward edge configurations, tapered ($\alpha = 45°$) and vertical ($\alpha = 90°$), and gusts of different durations (lengths) were investigated. The gusts were injected into the atmospheric boundary layer background flow on trajectories tilted by -45° to the horizontal. In the cases with gusts, fundamentally different flow phenomena at the canopy top in the forest edge region were observed compared to the atmospheric boundary layer flow alone. Upon impingement of an extreme gust on the forest edge, a clockwise rotating vortical motion (herein referred to as tertiary vortex) started to develop at the canopy top. The vortical motion translated downstream over the forest top and after a distance of approximately 2 tree heights h behind the forest edge, a patch with downward directed velocity appeared in its lee. This patch was responsible for the maximum downward transfer of horizontal and vertical momentum into the forest canopy. The location of the maximum downward transfer was between $1.25 < x/h < 1.75$ and was independent of the gust duration and the windward edge configuration. The magnitude of the downward momentum transfer, however, was dependent on the gust duration and the edge configuration. It increased with increasing gust duration and was larger for the forest canopy with a tapered edge in comparison to a vertical edge.

Introduction

Wind is responsible for more than 50% of the forest damage in Europe (e.g. Schelhaas et al. 2003, Gardiner et al. 2013). In particular so-called hundred-year storm events, e.g. hurricane *Lothar* in 1999 or hurricane *Kyrill* in 2007, have caused enormous destructions to European forests. Forest edge regions are especially prone and critical for forest stand stability. Initial storm-induced canopy gaps are likely to propagate into the forest interior and lead to extended damages.

Karlsruhe, Germany, ISBN 978-3-9816764-2-6

Recent research indicates that the interaction of the atmospheric boundary layer background flow with extreme gusts in the forest edge region can result in an augmented downward momentum transfer into the forest canopy which is presumably causal for the emergence of initial gaps (Tischmacher and Ruck 2013). This type of damage mechanism differs from former perceptions where the downward transfer of high momentum is attributed to coherent transverse roller structures which develop in the inflection layer in the forest canopy top and adjacent free air region (e.g. Raupach et al. 1996, Finnigan 2000, Finnigan et al. 2009). Since this mechanism is comparable to the formation of Kelvin-Helmholtz instabilities, it is termed mixing-layer analogy. However, the occurrence of extreme gusts originating from elevated parts of the atmospheric boundary layer, traveling downward and impinging on a forest canopy was recently observed by Träumner et al. 2012. In a field measurement campaign employing a scanning Doppler Lidar device, they identified such extreme gusts with scales of up to a few hundred meters in their records during the winter storm *Xynthia* in 2010 in south west of Germany.
In the current research project, the relationship between the characteristics of gusts imping on a windward edge, of atmospheric boundary layer background flows and the evolving momentum transfer at the canopy top is studied.

Material and Methods

Forest model

Wind tunnel experiments were performed at a reduced-scale forest model (1:200). Two windward forest edge configurations were realized, (i) a vertical edge (90°), and (ii) a tapered forest edge (45°). The forest model had a full-scale height of h = 22 m and extended 7 h in spanwise and 14 h in streamwise direction. It consisted of two distinct horizontal layers, the stem and the crown layer, both 11 m high (Figure 1). The stem layer was realized by ribbed cylindrical wooden dowels arranged in a staggered array. The crown layer was assembled from porous cones made of an open-porous foam material with 10 ppi (pores per inch) which mimicked the characteristic crown shape of needle trees. The aerodynamic similarity was based on the absorption of momentum from the flow. For the stem layer, the criterion involved the drag coefficient and the frontal area index of the tree stems. For the crown layer, the criterion relied on the pressure loss coefficient which describes the normalized continuous pressure decline of flow in a porous medium. The reader is referred to Gromke 2011, Gromke and Ruck 2012, and Gromke and Ruck 2015 for more detailed descriptions of the geometric and aerodynamic similarity criteria.

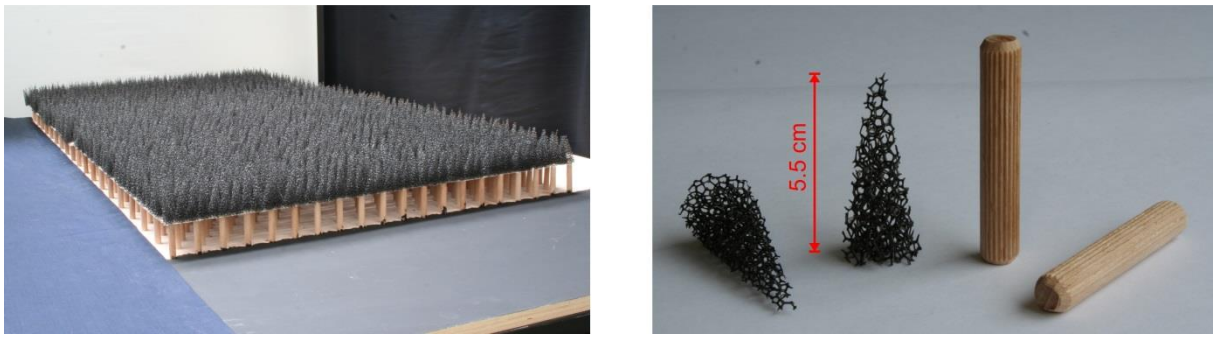

Figure 1: Forest model, single crown and stem model parts.

Simulated atmospheric boundary layer flow and generation of extreme gusts

A closed-circuit Goettingen-type wind tunnel with spires and ground-mounted roughness elements installed in the fetch windward of the test section generating a simulated atmospheric boundary layer flow was employed. The measurements were performed with a gradient velocity U_δ = 6.0 m/s and an aerodynamic roughness length z_0 = 0.0014 m. More details on the simulated atmospheric boundary layer flow can be found in Gromke and Ruck 2015. Assuming agricultural land use with mature crops (z_0 = 0.1 … 0.3 m) windward of the forest as it is typical for Central Europe, the geometric model scale M was determined to M = 1:200 (Wieringa 1993, WTG-Merkblatt 1995, Engineering Science Data Unit 2001).
The extreme gusts were generated by injecting pulsed round jets driven by compressed air into the simulated atmospheric boundary layer flow (background flow). The injection was controlled by a fast-switching solenoid valve (FESTO MHE4-MS1H-3/2G-QS-8-K). Full-scale gust durations of 4 and 12 seconds were realized. The extreme gusts entered the background flow through a straight long tube tilted by -45° to the horizontal with an initial full-scale diameter of 0.09 h at a position 2.8 h above the ground and 5 h in front of the vertical windward forest edge. The gusts entered the forest mainly through its windward edge with overspeeds of approximately factor 2 relative to the background flow while a smaller part of the gusts entered the forest from above through the canopy top.

Particle Image Velocimetry (PIV) system and measurement procedure

A 2D/2C TR PIV system from Dantec Dynamics was deployed for the measurements. The system consisted of a high-speed CMOS sensor with 1280 x 800 pixel resolution and a pulsed dual-cavity, frequency-doubled Nd:YAG laser, see Dantec Dynamics 2013 and Tischmacher and Ruck 2013 for more details. Recordings were made in the streamwise-oriented spanwise-central vertical plane (x-z) covering the forest edge region from $x^+ = x/h$ = -2.5 to x^+ = +6.0.
A PIV recording was synchronously started with the opening of the solenoid valve. The double-frame, single-exposure mode was employed with an inter-frame rate of 1000 Hz and intra-frame times of either 75 or 150 ns to ensure a time-resolved acquisition of the transient gust passage. The recordings were evaluated with DynamicStudio from Dantec Dynamics using a 2-step adaptive correlation algorithm including subpixel accuracy refinement (Dantec Dynamics 2013). The final interrogation window size was 32 x 32 pixel by 50% overlap along both dimensions resulting in a full-scale resolution of approximately 1-velocity-vector-per-square-meter. The recording procedure was repeated 50 times and the final evaluations as shown in the next chapter were based on 50 ensemble-averaged velocity field snapshots denoted by <>.

Results and Discussion

A set of 6 experiments was performed with variations in the windward edge taper angle α, 90° (vertical) and 45° (tapered), and variations in the gust duration T_g, 0 s (no gust), 4 s (short gust), and 12 s (long gust). The overpressure of the compressed air driving the gust injection into to the simulated atmospheric boundary layer background flow was the same for all experiments with superimposed gust (2 bar).

Karlsruhe, Germany, ISBN 978-3-9816764-2-6

Phenomenology of flow

Figure 2 shows the instantaneous distributions of the normalized wind speed $<|\vec{V}|>/<U_{ref}>$, with $<|\vec{V}|> = (<U>^2 + <W>^2)^{1/2}$, and of the normalized vertical velocity $<W>/<U_{ref}>$ for a sequence of (full-scale) time steps upon opening of the valve. $<U_{ref}>$ is the velocity of the undisturbed approach flow at tree height h. The snapshots were obtained with a gust duration $T_g = 4$ s at the forest model with vertical edge configuration ($\alpha = 90°$). Figure 3 shows the corresponding vorticity $<\omega>$ and swirling strength $<\lambda_{ci}^2>$ which is a criterion used to identify vortical structures in turbulent flows (Chong et al. 1990).

At $t_1 = 10$ s, the approaching gust before impinging on the windward forest edge can be seen. The gust front is approximately 1 h ahead of the forest edge and the flow field windward of the edge is not yet affected. Above the canopy top, an inclined layer which increases in thickness in flow direction of lower wind speed is apparent. The vertical velocity shows a pronounced downward flow in the core of the gust. Next to the gust core, a patch, centered at $x/h \approx -1.5$, $z/h \approx 1.5$, with upward directed flow is visible. The patch of upward directed flow is part of the closed ring vortex which is a secondary flow structure induced in the background flow due to the overspeed of the gust (Tischmacher and Ruck 2013). The illustration of the swirling strength $<\lambda_{ci}^2>$ clearly reveals the secondary flow structure in the streamwise-oriented spanwise-central vertical plane (x-z). The closed ring vortex has a counter-clockwise rotation in front / above the gust core and a clockwise rotation behind / below the gust core. The positive vertical velocity around the top of the forest edge reflects the upward deflection of the approach flow. The higher flow resistance in the forest canopy decelerates the wind and results in an upward flow component.

At $t_2 = 16$ s, the gust front starts to enter the forest through its windward edge. The swirling strength indicates that the ring vortex is still present although it is reduced in its strength. The upward flow around the top of the forest edge is clearly enhanced. This can be attributed to two reasons, (i) the increased volume flow coming with the gust and its upward deflection, and (ii) the contribution of the counter-clockwise rotating ring vortex section running ahead of the gust core with its upward directed flow motion. This section of the ring vortex induces a clockwise rotating tertiary vortex at the top of the forest canopy.

At $t_3 = 22$ s, approximately half of the gust has entered the forest canopy. An elongated patch with higher wind speed which is part of the gust is present directly above the forest top in the range $0.0 < x/h < 1.0$. It enters the forest through the canopy top as is indicated by the negative vertical velocity. The patch with positive vertical velocity has moved downstream and slightly upward. The counter-clockwise rotating section of the ring vortex and the induced clockwise rotating tertiary vortex are still present. They have moved downstream for a distance of approximately one tree height h.

At $t_4 = 30$ s, the wind speed directly above the forest top has increased up to a distance of 2 h behind the windward edge. A patch with negative vertical velocity is apparent at the canopy top in the range $1.0 < x/h < 1.5$. This patch is not a direct part of the extreme gust anymore as can be seen from intermediate snapshots between t_3 and t_4 (not shown here). Instead, between t_3 and t_4, the magnitude of the negative vertical velocity decreases before it increases again shortly before t_4. The reason for the decrease and the subsequent increase in the magnitude of the negative vertical velocity is not yet fully understood. It might be attributed to the vortical motion which becomes apparent in the swirling strength above the canopy top behind the forest edge in the range $0.0 < x/h < 1.0$. However, this patch leads to a local and timely restricted augmented momentum transport into the forest canopy because air with high speed from above the canopy is deflected downward. This observation seems to

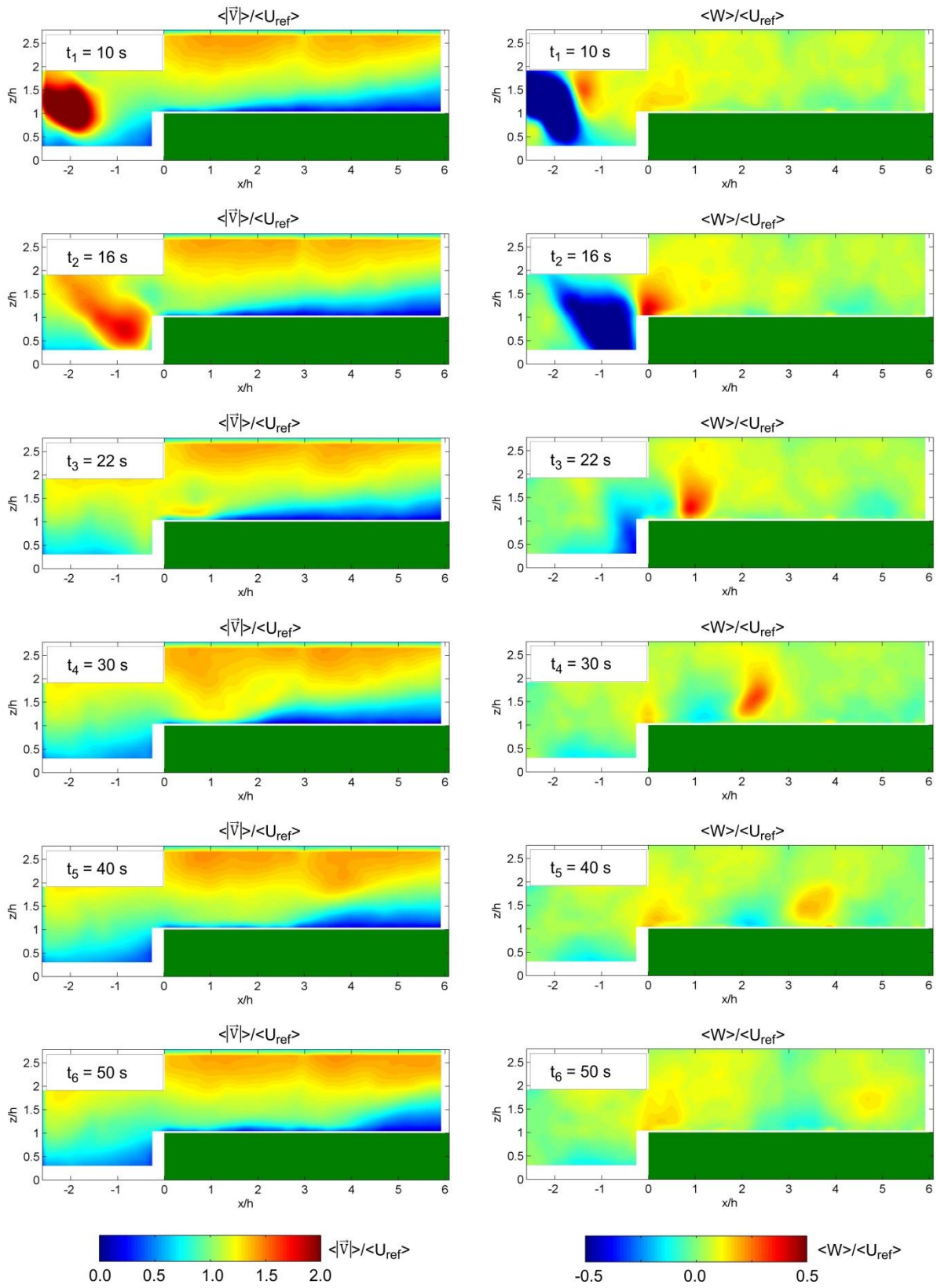

Figure 2: Ensemble-averaged instantaneous normalized wind speed $\langle|\vec{V}|\rangle/\langle U_{ref}\rangle$ and normalized vertical velocity $\langle W\rangle/\langle U_{ref}\rangle$ in the streamwise-oriented spanwise-central vertical plane (x-z) for full-scale gust duration T_g = 4 s at the forest model with vertical edge configuration (α = 90°).

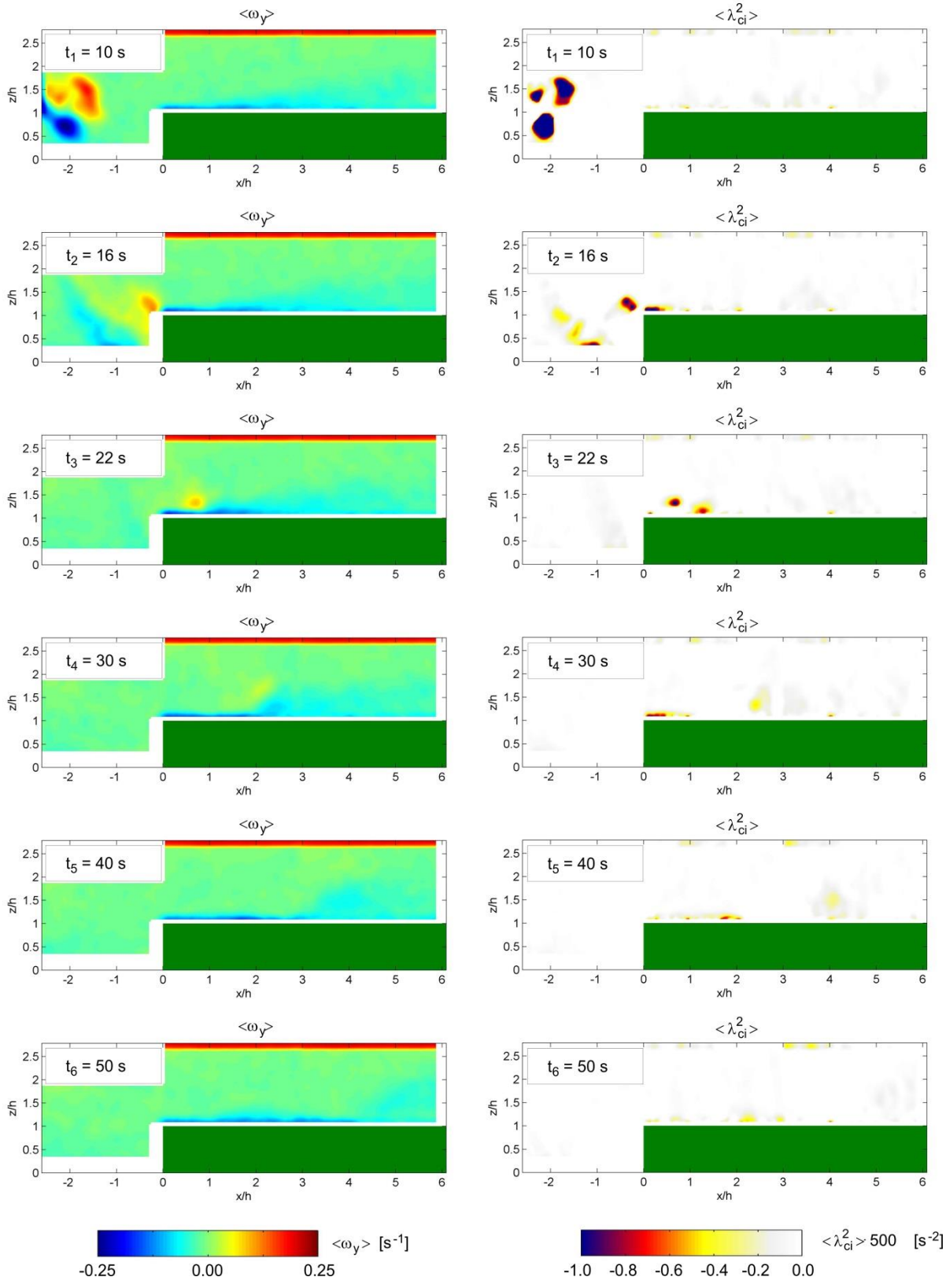

Figure 3: Ensemble-averaged instantaneous vorticity $\langle\omega_y\rangle$ and swirling strength $\langle\lambda_{ci}^2\rangle$ in the streamwise-oriented spanwise-central vertical plane (x-z) for full-scale gust duration T_g = 4 s at the forest model with vertical edge configuration (α = 90°).

differ from the findings of Tischmacher and Ruck 2013. However, they injected extreme gusts on horizontal trajectories into the background flow instead of on titled trajectories as is done here. They found an enhanced momentum transport into the forest canopy in front of the clockwise rotating tertiary vortex whereas here the enhanced downward transport occurs behind this vortex. The two different observations are not contradictory. They rather indicate a strong sensitivity of the flow phenomena and of the momentum transport into a forest canopy on the gust boundary conditions such as tilting angle and location of impingement at the forest edge.
At t_5 = 50 s and t_6 = 60 s, again patches with negative vertical velocity appear directly above the forest top. These patches have the potential for an increased downward momentum transport by entraining the air with high speed from directly above the canopy. An analysis of the intermediate snapshots from t_4 to t_5 and t_5 to t_6 (not shown here) reveals that the magnitude of the downward flow in these patches decreases temporarily before it increases again, i.e. the magnitude of the downward velocity shows an oscillating behavior.
Qualitatively comparable observations of the flow and vortex field characteristics at the canopy top were also made in the experiments with the long gust duration (12 s) and at the forest with tapered edge configuration (α = 45°). The development of a clockwise rotating tertiary vortex at the top of the forest edge upon approach of the counter-clockwise rotating section of the closed ring vortex, of a patch with negative vertical velocity changing in magnitude as it moves over the canopy top, and of the vortical motion at the forest top after the passage of the patch were also found. However, the flow and vortex structures differed quantitatively in their spatial extent and magnitude. The spatial extent of the patch with negative vertical velocity was larger in the experiment with the long gust duration and the magnitude of its downward velocity was also increased. A qualitative difference was observed in the secondary flow structure accompanying the core of the gust before impinging on the forest edge. Instead of one closed ring vortex as in the case of the short gust duration, consecutive ring vortices were indicated by the swirling strength in the case of the long gust duration.

Downward momentum transfer at the forest canopy top

Storm damage in forest stands behind the windward edge is attributed to downward transfer of momentum into the canopy. The resultant vertical transfer of momentum consists of two components (i) the downward transfer of horizontal momentum and (ii) the downward transfer of vertical momentum. Their fluxes (momentum per unit area and time) are given by $\rho \cdot W \cdot |U|$ and $\rho \cdot W \cdot |W|$, respectively. Figure 4 shows time histories of normalized kinematic vertical fluxes of horizontal and vertical momentum, I^+_{WU} and I^+_{WW} respectively, as well as of the total vertical flux of momentum $I^+_{tot} = I^+_{WU} + I^+_{WW}$ for various locations x/h behind the forest edge at height z = 1.14 h in the streamwise-oriented spanwise-central vertical plane (x-z). The data are based on the ensemble-averaged velocities <W> and <U> obtained at the forest model with vertical edge configuration (α = 90°) for a full-scale gust duration of T_g = 4 s.
Close to the windward edge (x/h ≤ 1.5), an initial upward directed total momentum flux occurs at the top of the forest canopy with the start of the gust passage. The upward flux is followed by a downward momentum flux. The period of the downward flux lasts 2.0 to 2.5 times longer than the upward one and increases in magnitude in streamwise direction. At x/h = 1.5 only a small upward flux is still apparent and the magnitude of the downward flux is maximum, i.e. the risk of storm damage by the downward transfer of momentum is largest in the region around 1.5 tree height h behind the windward edge. At locations x/h ≥ 2.0, the gust passage results solely in a downward transfer of momentum into the forest canopy which, however, decreases in magnitude with increasing x/h. The vertical transport of vertical mo-

mentum (ρ·W·IWI) is clearly smaller than the vertical transport of horizontal momentum (ρ·W·IUI). Its average contribution to the total vertical moment flux is 9.6%.

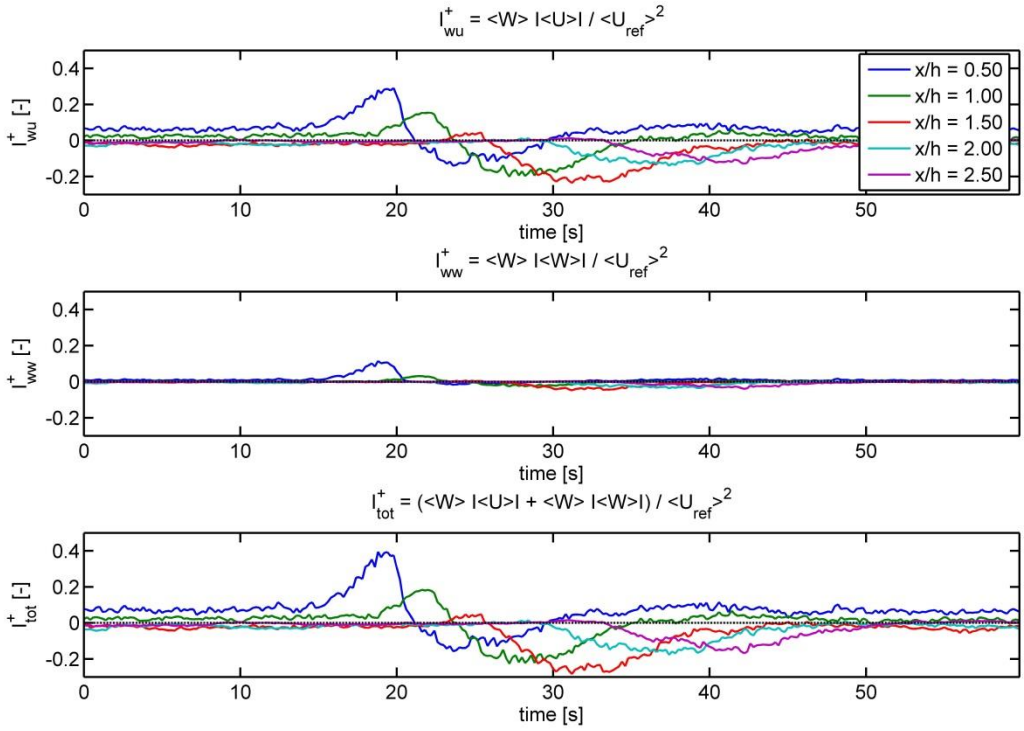

Figure 4: Normalized kinematic vertical fluxes of horizontal momentum I^+_{wu}, vertical momentum I^+_{ww} and total momentum I^+_{tot} at z = 1.14 h in the streamwise-oriented spanwise-central vertical plane (x-z) at the forest with vertical edge configuration (α = 90°) and full-scale gust duration T_g = 4 s.

The minimum normalized kinematic vertical fluxes of momentum $I^+_{WU,min}$, $I^+_{WW,min}$ and $I^+_{tot,min}$ at height z = 1.23 h along streamwise positions -2.0 < x/h < 6.0 are presented in Figure 5. The diagrams show data of all 6 experiments with different full-scale gust durations (T_G = 0, 4, 12 s) and taper angles of the windward forest edge (α = 45° or 90°).
The vertical momentum transport in the cases with gusts (T_G = 4 s or 12 s) differs characteristically from the cases without gusts (T_G = 0 s). In the latter, no downward transport of momentum into the forest canopy close to the edge (0.0 < x/h < 1.5) happens due to the upward deflection of the approach flow. For locations with x/h > 1.5, a comparatively small downward transport of momentum is present which is in general slightly larger in magnitude at the forest with tapered edge (α = 45°). In the cases with gusts, a downward transport of momentum can be noted in the forest edge region. The downward fluxes increase in magnitude in downstream direction and reach their minima between 1.25 < x/h < 1.75. An effect of the gust duration on the magnitude of the flux can be observed. The gusts with longer duration (T_G = 12 s) result in increased vertical downward fluxes. However, the location of the maximum downward transport is not notably affected by the gust duration. The tapered forest edge (α = 45°) results in an increased downward momentum transfer compared to the vertical edge (α = 90°). An analysis of the wind velocity components <U> and <W> at the canopy top during gust passages reveals that the horizontal velocity is unaffected by the taper angle while the maximum downward vertical velocity is larger in the case with tapered edge. This is attributed to a less steep upward deflection of the flow field because the atmospheric bound-

ary layer background flow and the superimposed gust “float more smoothly” over the tapered edge. The influence of the gusts on the minimum vertical momentum transport at the canopy top continues up to a distance of x/h ≈ 5.5 independent of their characteristics. For x/h > 5.5, the flux profiles collapse with those of the cases without gust.

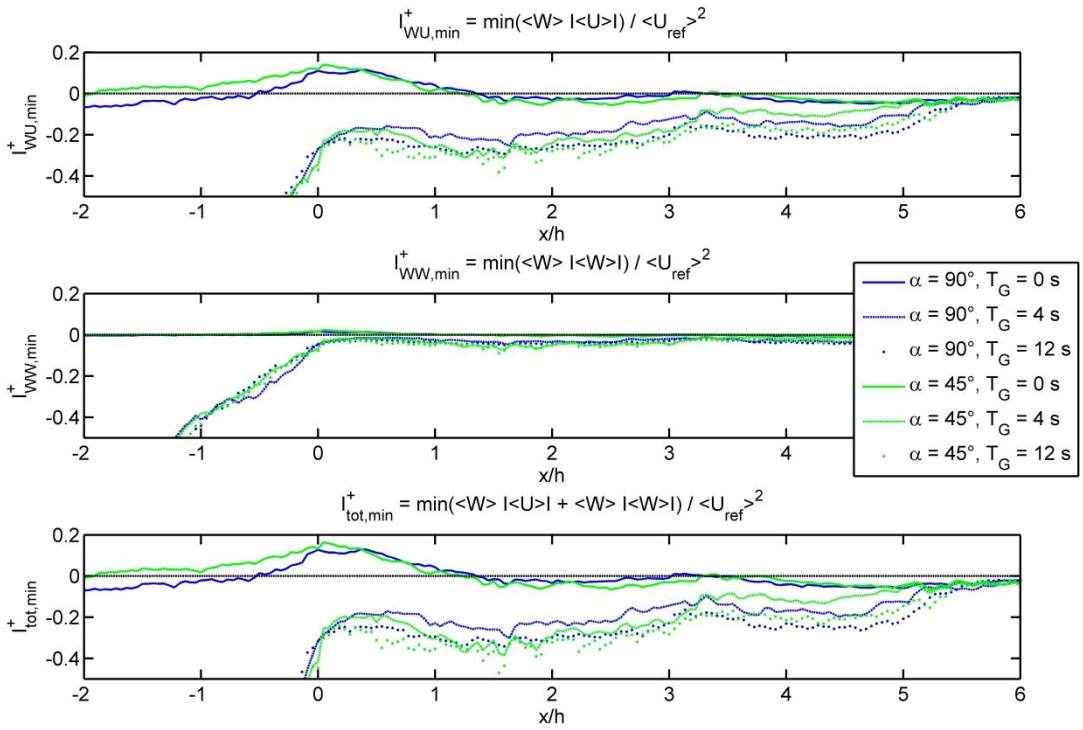

Figure 5: Minimum normalized kinematic fluxes of vertical momentum transport $I^+_{WU,min}$, $I^+_{WW,min}$ and $I^+_{tot,min}$ at height z = 1.23 h along streamwise positions -2.0 < x/h < 6.0 in the streamwise-oriented spanwise-central vertical plane (x-z) for various gust and taper angle characteristics.

Conclusions

In comparison with former observations made with gusts on horizontal trajectories by Tischmacher and Ruck 2013, the results of this study obtained with gusts on tilted trajectories show a dependency of the flow phenomena and of the momentum transport into a forest canopy on the tilting angle of the gust trajectories. The results of this study furthermore indicate that the taper angle of the forest edge and gust duration have an influence on the magnitude of the maximum downward momentum transfer into the canopy during a gust passage. Hence, the configuration of the edge is a measure to influence the storm stability of trees in forest stands at distances of one to two tree heights h behind the edge. Contrary to the intuitive expectation, the momentum transfer was larger in the case with tapered edge (α = 45°) than with vertical edge (α = 90°) during a gust passage. This observation suggests a careful approach when it comes to the design of forest edges. In particular it suggests the preference of a vertical edge over a tapered edge with α = 45° in terms of storm stability of trees at one to two tree heights h behind the edge. However, more edge configurations varying in taper angle, tree stand density and foliage density have to be investigated before final recommendations on optimal forest windward edge characteristics can be provided.

Acknowledgement

The financial support of the Deutsche Forschungsgemeinschaft DFG (German Research Foundation) under grant no. Ru 345/30-2 is gratefully acknowledged by the authors.

References

Chong, M.S., Perry, A.E., Cantwell, B.J., 1990: “A general classification of three dimensional flow fields”, Physics of Fluids A: Fluid Dynamics, Vol. 2, pp. 765-777
Dantec Dynamics, 2013: “DynamicStudio User’s Guide”, Version 3.40, pp.1- 660
Engineering Science Data Unit, 2001: “Characteristics of atmospheric turbulence near the ground - Part II”, ESDU 85020, pp. 1-42
Finnigan, J.J., 2000: “Turbulence in plant canopies”, Annual Review of Fluid Mechanics, Vol. 32, pp. 519-571
Finnigan, J.J., Shaw, R.H., Patton, E.G., 2009: “Turbulence structure above a vegetation canopy”, Journal of Fluid Mechanics, Vol. 637, pp. 387-424
Gardiner, B., Schuck, A., Schelhaas, M.-J., Orazio, C., Blennow, K., Nicoll, B. (editors), 2013: “Living with Storm Damage to Forests”, pp. 1-132
Gromke, C., 2011: “A vegetation modeling concept for Building and Environmental Aerodynamics wind tunnel tests and its application in pollutant dispersion studies”, Environmental Pollution, Vol. 159, pp. 2094-2099
Gromke, C., Ruck, B., 2012: “Pollutant concentrations in street canyons of different aspect ratio with avenues of trees for various wind directions”, Boundary-Layer Meteorology, Vol. 144, pp. 41-64
Gromke, C., Ruck, B., 2015: “Introduction of a new forest model for wind-tunnel studies and PIV-measurements of flow phenomena at the windward forest edge”, Proc. 23. GALA Fachtagung "Laser-methoden in der Strömungsmesstechnik", Dresden, Germany, Sep. 2014, pp. 43.1-43.8
Raupach, M.R., Finnigan, J.J., Brunet, Y., 1996: “Coherent eddies and turbulence in vegetation canopies: The mixing-layer analogy”, Boundary-Layer Meteorology, Vol. 78, pp. 351-382
Schelhaas, M.-J., Nabuurs, G.-J., Schuck, A., 2003: “Natural disturbances in the European forests in the 19th and 20th centuries”, Global Change Biology, Vol. 9, pp. 1620-1633
Tischmacher, M., Ruck, B., 2013: “Interaction of gusts and forest edges an experimental wind-tunnel study”, Forestry, Vol. 86, pp. 523-532
Träumner, K., Wieser, A., Ruck, B., Frank, C., Roehner, L., Kottmeier, C., 2012: “The suitability of Doppler lidar for characterizing the wind field above forest edges”, Forestry, Vol. 85, pp. 399-411
Wieringa, J., 1993: “Representative Roughness Parameters for Homogeneous Terrain”, Boundary-Layer Meteorology, Vol. 63, pp. 323-363
WTG-Merkblatt, 1995: “Windkanalversuche in der Gebäudeaerodynamik“, Windtechnologische Gesellschaft, pp. 1-43

Karlsruhe, Germany, ISBN 978-3-9816764-2-6